ELSEVIER

Polymer 43 (2002) 2031–2037

polymer

www.elsevier.com/locate/polymer

Ionic conduction of novel polymer composite films based on partially phosphorylated poly(vinyl alcohol)

Naomi Takada[a], Toshiki Koyama[a], Masahiro Suzuki[b,*], Mutsumi Kimura[a], Kenji Hanabusa[b], Hirofusa Shirai[a], Seizo Miyata[c]

[a]Department of Functional Polymer Science, Faculty of Textile Science and Technology, Shinshu University, Ueda, Nagano 386-8567, Japan
[b]Graduate School of Science and Technology, Shinshu University, Ueda, Nagano 386-8567, Japan
[c]Graduate School of Bio-application and Systems Engineering, Tokyo University of Agriculture and Technology, Koganei, Tokyo 184-8588, Japan

Received 6 September 2001; received in revised form 28 November 2001; accepted 6 December 2001

Abstract

New ion-conducting polymer composite films have been prepared, and their ionic conducting properties have been investigated. The polymer composite films are fabricated from partially phosphorylated poly(vinyl alcohol) with tetramethylammonium salt (P-PVA·Me_4N^+) and poly(acrylic acid) (PAA) or poly(ethylene glycol) (PEG). For P-PVA·Me_4N^+/PEG composite films, the ionic conductivity and carrier density sharply increased, and carrier mobility sharply decreased around $[PEG]/[PO_3]_{P\text{-}PVA}$ of 2. The ionic conductivity is dominated by both carrier density and carrier mobility at $[PEG]/[PO_3]_{P\text{-}PVA} < 2$ and only by carrier density at $[PEG]/[PO_3]_{P\text{-}PVA} > 2$. This is attributed to the fact that the ionic conduction in P-PVA·Me_4N^+/PEG composite films occurred through the PEG–Me_4N^+ complex which was independent of the carrier mobility. On the other hand, the ionic conductivity in P-PVA·Me_4N^+/PAA composite films showed a bell-shaped dependence on the PAA contents with a maximum value at $[CO_2H]_{PAA}/[OH]_{P\text{-}PVA} = 1$. FTIR spectrum measurements demonstrated that part of the carboxylic acid residues was dissociated in the composite films. This fact implied that the ionic conduction was mediated by PAA at the low PAA content. At high PAA content, however, an excess of the carboxylic acid residues formed trapping sites for the Me_4N^+ ion, leading to a decrease in the ionic conductivity. Furthermore, we proposed a unique mechanism of the ionic conduction.

Keywords: Ionic conduction; Polymer composite; Partially phosphorylated poly(vinyl alcohol)

1. Introduction

Ionically conducting polymers have been of considerable interest because of their potential application as a polymer solid electrolyte. The polymer solid electrolytes have attracted great scientific interest during the last two decades due to their many advantages such as high energy density, electrochemical stability and easy handling [1–2]. Poly(ethylene oxide)-based complexes acting as polymer electrolytes have been widely used [2–5]. However, there are several disadvantages in using PEO: the major drawback is easy crystallization of PEO or the formation of crystalline complexes resulting in a dramatic decrease in ionic conductivity. In order to solve this problem, many approaches have been carried out to reduce the crystallinity of PEO-based electrolytes and increase the segmental mobility of the host polymer: e.g. polyphosphazene [6–7], poly(itaconate) with side-chain-grafted PEO [2], and poly(vinylidene fluoride) [8], poly(acrylonitrile) [9–11], poly(methyl methacrylate) [12], poly(vinyl pyrrolidone) [13], and poly(ethyleneglycol diacrylate) [14] plasticized with ethylene carbonate, propylene carbonate, or a mixture of ethylene carbonate and propylene carbonate. These polymers have the mechanical stability and these polymer solid electrolytes containing cations such as lithium and alkylammonium ions provide relatively high ionic conductivities.

Recently, we have reported proton conduction in cross-linking partially phosphorylated poly(vinyl alcohol) (P-PVA) hydrogel films and demonstrated that the hydrogel films are relatively good polymer gel electrolytes [15]. Quite recently, cation conduction in the P-PVA film has been investigated [16]. In the present paper, the composite films of P-PVA with tetramethylammonium salt and poly(acrylic acid) (PAA) or poly(ethylene glycol) (PEG) are

---

* Corresponding author. Address: Department of Functional Polymer Science, Faculty of Textile Science and Technology, Shinshu University, Ueda, Nagano 386-8567, Japan. Fax: +81-268-24-7248.
E-mail address: msuzuki@giptc.shinshu-u.ac.jp (M. Suzuki).

0032-3861/02/$ - see front matter
PII: S0032-3861(01)00801-1

fabricated, and the effects of PAA and PEG on ionic conduction are investigated.

2. Experimental

2.1. Materials

Poly(vinyl alcohol) (PVA: MW = 2000, Pn = ca. 45) used in these experiments was an analytical grade of commercial origin and was completely hydrolyzed by alkali in methanol. *N*,*N*-dimethylformamide (DMF) was purified by double distillation under reduced pressure just before use. Poly(acrylic acid) (PAA: MW = 25 000, Pn = ca. 350), poly(ethylene glycol) (PEG: MW = ca. 200, Pn = 4.5) and all of the other reagents were commercially available guaranteed reagents and were used without further purification. Partially phosphorylated PVA with dipotassium salt (P-PVA·K^+) was prepared according to Refs. [15,16]. P-PVA with tetramethylammonium salt (P-PVA·Me_4N^+) was obtained by ion exchange reaction from proton to tetramethylammonium ion. The proton-type P-PVA was dissolved in water, and an aqueous solution of tetramethylammonium hydroxide was added until the pH became ca. 11. After stirring for 24 h, P-PVA·Me_4N^+ was obtained by reprecipitation into acetone. The degree of phosphorylation for the P-PVA obtained was determined to be 0.22 by pH titration and the molybdenum blue method. The chemical structure of P-PVA is shown in Fig. 1.

Polymer sample solutions were prepared as follows. P-PVA was dissolved in distilled water, and PAA or PEG was added under the conditions of various molar ratios of carboxylic acid residue in PAA or ethylene glycol unit to the hydroxyl group in the P-PVA unit. The ratios are $[–CO_2H]/[–PO_3] = 0$, 0.5, 1.0, 1.5 and 2.0 for PAA composite films and $[PEG]/[–PO_3] = 0–4$.

The standard devices were prepared by casting the sample solution on an ITO electrode. Sample solutions were sandwiched between two ITO electrodes which were coated with acrylic resin and then slowly dried on P_2O_5.

2.2. Measurements

Fourier-transform infrared (FTIR) spectra of the sample films were measured using a JASCO FT/IR-7300 Fourier-Transform Infrared spectrophotometer. Thermal analyses were performed using SEIKO DSC 15200 instrument systems, consisting of thermogravimetric analysis, differential thermal analysis (TG/DTA 220) and DSC 220 instruments. DSC measurements were carried out at a heating rate of 10 °C min^{-1} over a temperature range of −120 to +300 °C. Ionic conductivities of the sample films which were sufficiently dried at 50 °C in 10^{-5} Torr for 24 h were determined from complex impedance plots obtained using a Hewlett Packard 4192A LF impedance analyzer over the frequency range of 5 Hz to 13 MHz. The temperature dependence of the ionic conductivity was carried out in the temperature range from 15 to 60 °C. The carrier mobility and density of the films were determined by DC polarization measurements using a Yanako polarographic analyzer P-1100 and a Watanabe XY-recorder WX4421. After application of a fixed voltage of +1.0 V to the sample films for 1 h, the transient current value which correlated between current and time was recorded until the current reached a steady state. The carrier mobility (μ_+) and carrier density (N_{0+}) are, respectively, given by the slope and intercept of plotting according to Eq. (1) [17].

$$\ln I(t) = \ln\left[\frac{SN_{0+}q\mu_+V}{d}\right] - \left[\frac{\mu_+V}{d^2}\right]t \qquad (1)$$

where S is the electrode area, q is the charge of the cation, V is the applied voltage, and d is the thickness of the film.

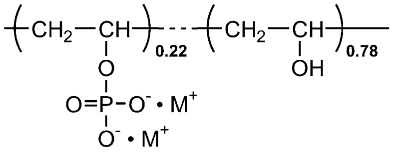

$$-\!\left(CH_2-\underset{\underset{O=\underset{\underset{O^-\cdot M^+}{|}}{P}-O^-\cdot M^+}{|}}{\underset{O}{|}}{CH}\right)_{0.22}\cdots\left(CH_2-\underset{OH}{\underset{|}{CH}}\right)_{0.78}\!-$$

$M^+ = K^+$	P-PVA • K^+
$M^+ = Me_4N^+$	P-PVA • Me_4N^+

Fig. 1. Chemical structure of P-PVA.

3. Results and discussion

3.1. Ionic conduction and thermal properties of P-PVA·Me_4N^+ and P-PVA·K^+ films

Fig. 2 shows the temperature dependence of ionic conductivities in P-PVA·K^+ and P-PVA·Me_4N^+ films. Experimental data in relation to these films are summarized in Table 1. The ionic conductivity in the P-PVA·Me_4N^+ film was increased about one order of magnitude over that in the P-PVA·K^+ film. Furthermore, the carrier mobility

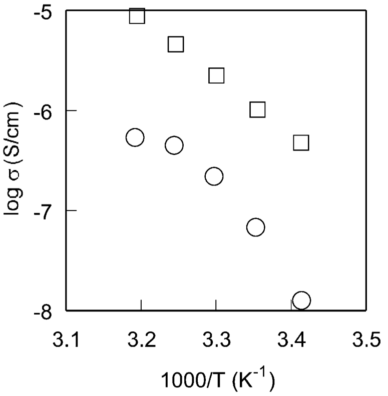

Fig. 2. Temperature dependence of ionic conductivities of P-PVA·K^+ (○) and P-PVA·Me_4N^+ (□) films.

Table 1
Experimental data for P-PVA·K^+ and P-PVA·Me_4N^+ films

	log σ (S cm^{-1})[a]	log $(\mu_+)_{app}$ (cm^2 V^{-1} s^{-1})[b]	log $(N_{0+})_{app}$ (cm^3)[c]	E'_a (eV)[d]	T_g (K)[e]
P-PVA·K^+ film	−6.64	−6.32	16.1	1.22	207
P-PVA·Me_4N^+ film	−5.63	−2.68	15.1	0.211	233

[a] Ionic conductivity at 303 K.
[b] Apparent carrier mobility at 303 K.
[c] Apparent carrier density at 303 K.
[d] Activation energy obtained from Eq. (4).
[e] Glass transition temperature.

P-PVA·Me_4N^+ film was significantly enhanced with decreasing the activation energy in spite of a decrease in the carrier density. These facts indicate that the large ionic conductivity in the P-PVA·Me_4N^+ film is caused by the large carrier mobility. Compared with a potassium cation, a tetramethylammonium cation has a large hydrophobicity and small interaction with polar residues on the polymer such as hydroxyl and phosphate groups, which leads to easy ionic conduction. This is supported by the fact that the activation energy for ionic conduction in the P-PVA·Me_4N^+ film is about 6-fold smaller than that in the P-PVA·K^+ film. We did not study the P-PVA·K^+ film in detail.

3.2. Thermal properties of composite films

The experimental data obtained from DSC measurements of P-PVA·Me_4N^+ composite films with PEG or PAA are listed in Table 2. The glass transition temperature, T_g, decreased with increasing PEG contents in P-PVA·Me_4N^+/PEG composite films, while such the behavior was not detected in the P-PVA·Me_4N^+/PAA composite films. It has been known that PEG acts as a plasticizer [18–19] and that PEG interacts with the P-PVA backbone through hydrogen bonding between polar ether groups in the main chain of PEG and hydroxyl groups on P-PVA. The hydrogen bonding induces the expansion of the P-PVA chains, and the amorphous part of the films increases with added PEG, therefore leading to the T_g reduction. On the other hand, the T_g of the P-PVA·Me_4N^+/PAA composite films is difficult to detect. PAA also undergoes hydrogen bonding between the carboxylic acid groups on PAA and the hydroxy groups on P-PVA [20]. Therefore, this might be attributed to the fact that the P-PVA chains are fixed on the PAA chains through the hydrogen bonding.

Table 2
Activation energy for ionic conduction and glass transition temperature (T_g) of composite films

	Ratio[a]	E'_a[b] (eV)	T_g (K)
P-PVA·Me_4N^+/PEG-1	1.33	0.196	223
P-PVA·Me_4N^+/PEG-2	1.78	0.184	214
P-PVA·Me_4N^+/PEG-3	2.22	0.171	207
P-PVA·Me_4N^+/PEG-4	2.53	0.175	202
P-PVA·Me_4N^+/PEG-5	3.93	0.177	198
P-PVA·Me_4N^+/PAA-1	0.5	0.187	–[c]
P-PVA·Me_4N^+/PAA-2	1.0	0.172	–[c]
P-PVA·Me_4N^+/PAA-3	1.5	0.164	–[c]
P-PVA·Me_4N^+/PAA-4	2.0	0.165	–[c]

[a] $[PEG]/[PO_3]_{P\text{-}PVA}$ for PEG composite films and $[CO_2H]_{PAA}/[OH]_{P\text{-}PVA}$ for PAA composite films.
[b] Activation energy obtained from Eq. (4).
[c] Not detected.

3.3. Ionic conduction in P-PVA·Me_4N^+/PEG composite films

Fig. 3 shows the effects of PEG on the ionic conductivity at 298, 303 and 313 K. The ionic conductivity increased with increasing temperature. For all temperatures, the ionic conductivity was hardly affected by PEG at $[PEG]/[PO_3]_{P\text{-}PVA} < 2$ and then slightly increased at $[PEG]/[PO_3]_{P\text{-}PVA} > 2.4$, through a sharp increase around $[PEG]/[PO_3]_{P\text{-}PVA}$ of 2. Such a sharp change suggests that the mechanism of the ionic conduction varies with the addition of PEG, particularly around $[PEG]/[PO_3]_{P\text{-}PVA}$ of 2. To solve this problem, the temperature dependence of the ionic conductivity was carried out. The temperature dependence of the ionic conductivity provides an important information on the mechanism of the ion conduction. Fig. 4 shows the temperature dependence of the ionic conductivities in P-PVA·Me_4N^+/PEG composite films with $[PEG]/[PO_3]_{P\text{-}PVA}$ of 0, 1.33, 1.78, 2.22, 2.53 and 3.93. It is clear that the temperature dependence also changed around $[PEG]/[PO_3]_{P\text{-}PVA}$ of 2. The temperature dependence of the ionic conductivity shows an upward curve for all systems. The ionic conduction in the polymer electrolytes depends on the segmental motion of the polymers, and the temperature dependence shows non-linear plots [2,15]. In the present case, the ionic conduction is affected by the segmental motion of the P-PVA chains. However, the temperature dependence shows a clear upward curve at $[PEG]/[PO_3]_{P\text{-}PVA} < 2$ and approaches a straight line at $[PEG]/[PO_3]_{P\text{-}PVA} \geq 2$.[1] This result provides evidence of a change in the mechanism of the ionic conduction around $[PEG]/[PO_3]_{P\text{-}PVA} = 2:$ the ionic conduction is affected

---

[1] In the present cases, the plots became the complete linear even at $[PEG]/[PO_3]_{P\text{-}PVA} = 3.9$.

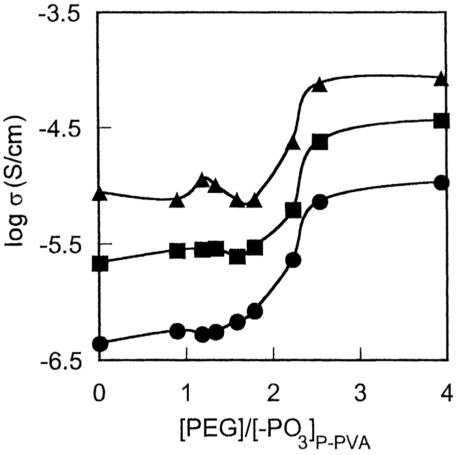

Fig. 3. PEG effects on ionic conductivities of P-PVA·Me$_4$N$^+$/PAA composite film at 298.15 K (●), 303.15 K (■), and 313.15 K (▲).

by the segmental motion of P-PVA chains at $[PEG]/[PO_3]_{P\text{-}PVA} < 2$, whereas the influence of the segmental motion decreases at $[PEG]/[PO_3]_{P\text{-}PVA} \geq 2$. In particular, the ionic conductivity is little affected by the segmental motion at $[PEG]/[PO_3]_{P\text{-}PVA} = 3.9$. Thus, the ionic conduction tends to change from Williams–Landel–Ferry (WLF) [21] to Arrhenius type.

Since the present temperature dependence of the ionic conductivity was not Arrhenius type. The activation energy for ionic conduction was analyzed using a WLF equation and modified Vogel–Tamman–Fulcher (VTF) equation [22].

WLF equation

$$\log\left[\frac{\sigma(T)}{\sigma(T_g)}\right] = \left[\frac{C_1(T-T_g)}{C_2(T-T_g)}\right] \tag{2}$$

$$y = \left\{\log\left[\frac{\sigma(T)}{\sigma(T_g)}\right]\right\}^{-1} = \frac{C_2 x}{C_1} + \frac{1}{C_1}, \qquad x = (T-T_g)^{-1} \tag{3}$$

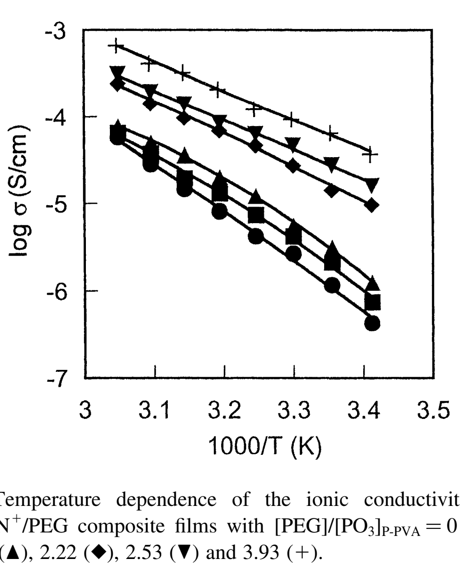

Fig. 4. Temperature dependence of the ionic conductivities in P-PVA·Me$_4$N$^+$/PEG composite films with $[PEG]/[PO_3]_{P\text{-}PVA} = 0$ (●), 1.33 (■), 1.78 (▲), 2.22 (◆), 2.53 (▼) and 3.93 (+).

VTF equation

$$\sigma = A' \exp\left[\frac{-E'_a}{k(T-T'_0)}\right] \tag{4}$$

$$\log\sigma = \left[\frac{-E'_a}{2.303(T-T'_0)}\right] + \log A', \qquad T'_0 = T_g - C_2 \tag{5}$$

where T_g is the glass transition temperature, E'_a is the activation energy, and T'_0 is the thermodynamic ideal glass transition temperature at which the configurational entropy becomes zero or the free volume disappears. The activation energy obtained is listed in Table 2. With increasing PEG content, the activation energy decreases up to $[PEG]/[PO_3]_{P\text{-}PVA}$ of 2 and then is almost constant at $[PEG]/[PO_3]_{P\text{-}PVA} \geq 2$. This result agrees with that of the T_g; the activation energy decreases accompanying a decrease in the T_g; therefore, the ionic conductivity is increased by the decrease in the activation energy.

In general, it is known that the ionic conductivity is determined by the carrier density and mobility. To consider this in more detail, the carrier density and carrier mobility were estimated from DC polarization measurements. Here, carrier density and carrier mobility obtained are apparent values. Fig. 5 shows the dependence of apparent carrier density and apparent carrier mobility on the PEG content at 298 K. With increasing PEG content, the carrier density gradually increased at $[PEG]/[PO_3]_{P\text{-}PVA} < 1.5$ and $[PEG]/[PO_3]_{P\text{-}PVA} > 2.4$, through a sharp increase around $[PEG]/[PO_3]_{P\text{-}PVA}$ of 2. The carrier mobility also showed a sharp decrease around $[PEG]/[PO_3]_{P\text{-}PVA}$ of 2, and it slightly decreased at $[PEG]/[PO_3]_{P\text{-}PVA} < 2$. Surprisingly, the ionic conductivity, carrier density and carrier mobility significantly change with increasing PEG content around $[PEG]/[PO_3]_{P\text{-}PVA}$ of 2. These results indicate that the ionic conductivity is determined by both the carrier density and carrier

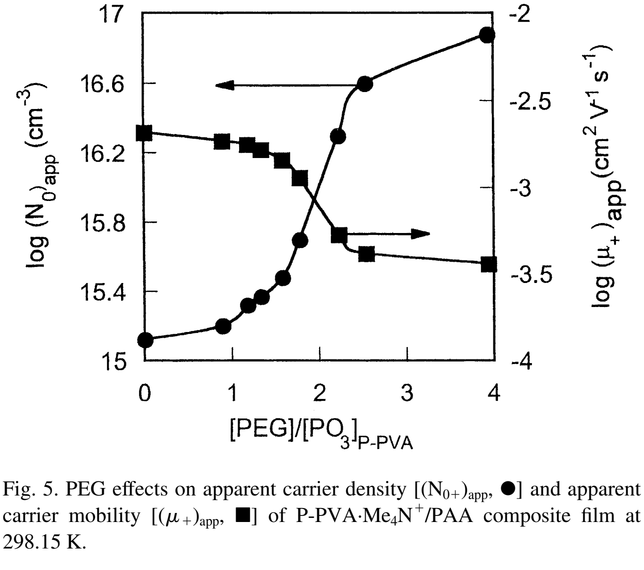

Fig. 5. PEG effects on apparent carrier density [$(N_{0+})_{app}$, ●] and apparent carrier mobility [$(\mu_+)_{app}$, ■] of P-PVA·Me$_4$N$^+$/PAA composite film at 298.15 K.

mobility at $[\mathrm{PEG}]/[\mathrm{PO_3}]_{\text{P-PVA}} < 2$ and that it is mainly dominated by the carrier density. At $[\mathrm{PEG}]/[\mathrm{PO_3}]_{\text{P-PVA}} < 2$, the carrier density increases and the carrier mobility decreases; the ionic conductivity remains almost constant. This is the reason why the enhancement effect of the carrier density on the ionic conductivity balances the decrease in the carrier mobility. The PEG content-dependence of the ionic conductivity is very similar to that of the carrier density at $[\mathrm{PEG}]/[\mathrm{PO_3}]_{\text{P-PVA}} \geq 2$. The decrease in the carrier mobility is likely compensated by the increase in the carrier density.

As mentioned earlier, PEG undergoes hydrogen bonding with P-PVA chains. Moreover, it is known that PEG easily solvates cations by interaction with the ether groups on PEG and can coordinate effectively with cations [23]. Considering these facts, the change in the microstructure of the P-PVA·$\mathrm{Me_4N^+}$/PEG composite film with the addition of PEG is assumed as follows. At $[\mathrm{PEG}]/[\mathrm{PO_3}]_{\text{P-PVA}} < 2$, the addition of PEG expands the entwining chains in the random coil structure of P-PVA and increases the number of conducting carriers; therefore, the carrier density increases. The carrier mobility decreases because the hydrogen bonding between P-PVA chains and PEG restricts the segmental motion of the P-PVA backbone, which is supported by the upward temperature-dependence of the ionic conductivity. With further adding of PEG, PEG would form the complex with cations, referred to as PEG–$\mathrm{Me_4N^+}$. In general, it has been known that PEG accelerates the dissociation of alkali metal salts such as lithium and sodium [24,25]. In our cases, PEG promotes the formation of the $\mathrm{Me_4N^+}$ ion, and PEG–$\mathrm{Me_4N^+}$ complexes are formed by PEG which may undergo no interaction with P-PVA chains, consequently leading to a further increase in the carrier density. The sharp decrease in the carrier mobility is caused by the formation of PEG–$\mathrm{Me_4N^+}$ complexes: this may be attributed to the fact that the PEG–$\mathrm{Me_4N^+}$ complex has a larger molecular size than $\mathrm{Me_4N^+}$. However, the carrier mobility hardly influences the ionic conductivity.

3.4. Ionic conduction of P-PVA·$\mathrm{Me_4N^+}$/PAA composite films

Fig. 6 shows the PAA effects on the ionic conductivity of P-PVA·$\mathrm{Me_4N^+}$/PAA composite films at 298 K. With increasing PAA content, the ionic conductivity increased up to $[\mathrm{CO_2H}]_{\text{PAA}}/[\mathrm{OH}]_{\text{P-PVA}} = 1$ and then decreased; namely, the composite film, prepared from a mixture of P-PVA·$\mathrm{Me_4N^+}$ and PAA with 1:1, gave the highest ionic conductivity. Such a bell-shaped dependence indicates that the ionic conductivity is affected by at least two factors, which enhance and decrease the ionic conductivity. To obtain information on the mechanism, the temperature dependence of the ionic conductivity was carried out and the results are shown in Fig. 7. The temperature dependence shows an upward curve for all PAA content systems, indicating the WLF type of the ionic conduction. Therefore, the ionic conduction is affected by the segmental motion of P-PVA chains. Using Eqs. (2)–(5), the activation energies of the ionic conduction are estimated for P-PVA·$\mathrm{Me_4N^+}$/PAA composite films and are listed in Table 2. The activation energy decreases with increasing PAA content. At high PAA content, however, the ionic conductivity is low, in spite of the low activation energy.

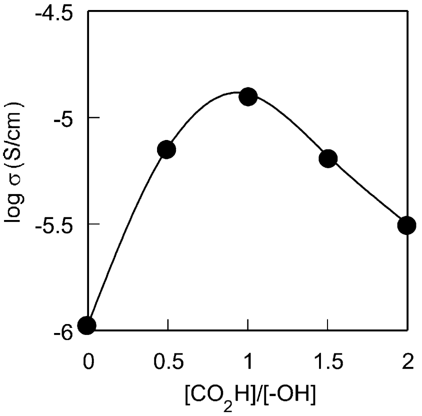

Fig. 6. PAA effects on ionic conductivity of P-PVA·$\mathrm{Me_4N^+}$/PAA composite film at 298.15 K.

Fig. 8 shows the dependence of apparent carrier density and apparent carrier mobility on the PAA contents in P-PVA·$\mathrm{Me_4N^+}$/PAA composite films. The carrier density increased up to $[\mathrm{CO_2H}]_{\text{PAA}}/[\mathrm{OH}]_{\text{P-PVA}}$ of 1.5 and then decreased. The carrier mobility slightly increased and then sharply decreased at $[\mathrm{CO_2H}]_{\text{PAA}}/[\mathrm{OH}]_{\text{P-PVA}} > 1.0$. Such the bell-shaped PAA content-dependence of the ionic conductivity can be explained as follows. At $[\mathrm{CO_2H}]_{\text{PAA}}/[\mathrm{OH}]_{\text{P-PVA}} < 1.0$, both the carrier mobility and carrier density increase. Because the PAA content-dependence of carrier density is very similar to that of the ionic conductivity, however, the ionic conductivity is mainly dominated by the carrier density. At $[\mathrm{CO_2H}]_{\text{PAA}}/$

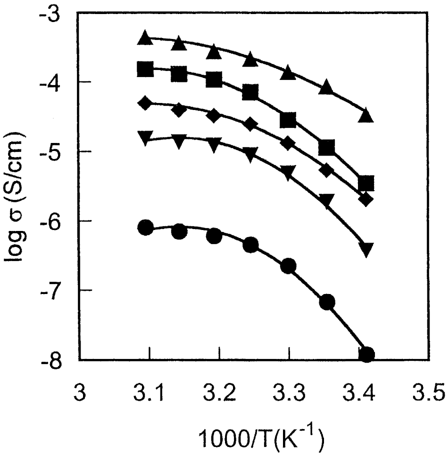

Fig. 7. Temperature dependence of the ionic conductivities in P-PVA·$\mathrm{Me_4N^+}$/PAA composite films with $[\mathrm{CO_2H}]_{\text{PAA}}/[\mathrm{OH}]_{\text{P-PVA}} = 0$ (●), 0.5 (■), 1.0 (▲), 1.5 (◆), and 2.0 (▼).

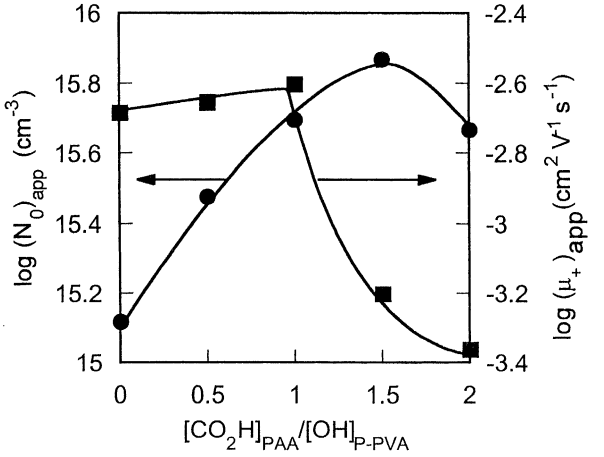

Fig. 8. PAA effects on apparent carrier density [$(N_{0+})_{\mathrm{app}}$, ●] and apparent carrier mobility [$(\mu_+)_{\mathrm{app}}$, ■] of P-PVA·Me_4N^+/PAA composite film at 298.15 K.

$[OH]_{P\text{-}PVA} > 1.0$, it is clear that the ionic conductivity is dominated by the carrier mobility. Part of the hydroxyl residues and carboxylic acid residues participates in the hydrogen bonding because of their structures: PAA and P-PVA have a random coil structure which are a mixed structure of the expanded chains and compactly entwining chains. The hydrogen bonding forms between both the expanded chain portions. Practically, the cations on the expanded portions of P-PVA conduct, but those on the compactly entwining portions do not because of steric hindrance. With added PAA, the hydrogen bonding formed around the expanded portions would induce further expansion of the compactly entwining portions on the P-PVA chains. The carrier density increases with increasing of the expanded portion on the P-PVA.

The carrier mobility is barely affected by PAA at $[CO_2H]_{PAA}/[OH]_{P\text{-}PVA} < 1.0$ and sharply decreases at $[CO_2H]_{PAA}/[OH]_{P\text{-}PVA} > 1.0$. The segmental motion (equivalent to flexibility) of the P-PVA chains significantly depends on the hydrogen bonding with PAA. However, the expansion of the P-PVA chains, induced by the hydrogen bonding with PAA, slightly increases the flexibility of the P-PVA chains even when the PAA content is low ($[CO_2H]_{PAA}/[OH]_{P\text{-}PVA} < 1$), because the PAA also interacts with the expanded portions of P-PVA through hydrogen bonding. Consequently, the expansion effect on the carrier mobility is very small. At $[CO_2H]_{PAA}/[OH]_{P\text{-}PVA} > 1$, many hydrogen bonding portions significantly restrict the flexibility of the P-PVA chains, leading to a sharp decrease in the carrier mobility.

Furthermore, FTIR spectrum measurements of the P-PVA·Me_4N^+/PAA composite films revealed an interesting result. Absorption bands at 1561, 1406, and 925 cm^{-1}, assigned to the carbonyl group of the carboxylate ion on PAA, in addition to at 1701 and 1176 cm^{-1}, assigned to the carbonyl group of the carboxylic acid residue, were observed. These implied that the ionic conduction in P-PVA·Me_4N^+/PAA composite films is mediated by the carboxylic acid and/or carboxylate groups on PAA. In the present system, ionic conduction takes place through hopping of cations between phosphorylate residues. As mentioned earlier, PAA undergoes hydrogen bonding with P-PVA chains; namely, these form a polymer complex in the composite films. Many carboxylic acid residues are placed around and between the phosphorylate residues. Probably, the carboxylic acid and carboxylate residues form an ionically conducting path and mediate the Me_4N^+ ion transport, which leads to the increase in the carrier mobility and the decrease in the activation energy. Therefore, the ionic conductivity also increases by the mediated effect as well as the increase in carrier density and carrier mobility at $[CO_2H]_{PAA}/[OH]_{P\text{-}PVA} < 1$. The ionically conducting path would also be formed at $[CO_2H]_{PAA}/[OH]_{P\text{-}PVA} > 1$. However, an excess of carboxylic acid residues, not participating in interaction with the P-PVA chains, forms aggregates and a trapping site arises which traps Me_4N^+ ions and inhibits the ionic conduction. In particular, the trapping is large at $[CO_2H]_{PAA}/[OH]_{P\text{-}PVA} = 2$, as supported by the fact that the carrier density and carrier mobility decrease at high PAA content. Consequently, the ionic conductivity is low in spite of the low activation energy.

4. Conclusions

We revealed the effects of PEG and PAA on the ionic conduction of the P-PVA·Me_4N^+/PEG and P-PVA·Me_4N^+/PAA composite films. By blending PEG and PAA into P-PVA·Me_4N^+, the ionic conductivity is increased. For P-PVA·Me_4N^+/PEG, the mechanism of the ionic conduction changes with the addition of PEG, particularly around $[PEG]/[PO_3]_{P\text{-}PVA}$ of 2. The ionic conduction is affected by the segmental motion of the P-PVA chains at $[PEG]/[PO_3]_{P\text{-}PVA} < 2$ but is little affected at $[PEG]/[PO_3]_{P\text{-}PVA} > 2$. This is attributable to the formation of a complex of Me_4N^+ ion with PEG (PEG–Me_4N^+) at the high PEG content. On the other hand, the ionic conductivity is increased by blending PAA because the carboxylic acid and/or carboxylate residues form an ionically conducting path which mediates the ionic conduction. At the high PAA content, however, an excess of carboxylic acid residues forms a trapping site which restricts the Me_4N^+ ion conduction, leading to a decrease in the ionic conductivity.

Acknowledgements

This work was supported by a Grant-in-Aid for COE Research (10CE2003) by the Ministry of Education, Culture, Sports, Science and Technology of Japan.

References

[1] Armand MB. Solid State Ionics 1994;69:309.
[2] MacCallum JR, Vincent CA. Polymer electrolyte reviews 1 and 2. London: Elsevier, 1987 and 1989.
[3] Wright PV. Br Polym J 1975;7:319.
[4] Takeoka S, Ohno H, Tsuchida E. Polym Adv Technol 1993;4:53.
[5] del Rio C, Acosa JL. Polym Bull 1997;63:39.
[6] Blonsky PM, Shriver DF, Allcock HR, Austin P. J Am Chem Soc 1984;106:6854.
[7] Tada Y, Sato M, Takeno M, Kameshima T, Nakacho Y, Shigehara K. Macromol Chem Phys 1994;195:571.
[8] Tsuchida E, Kobayashi N, Ohno H. Electrochim Acta 1983;28:591.
[9] Croce F, Gerace F, Dautzemberg G, Passerini S, Appetecchi GB, Scrosati B. Electrochim Acta 1994;39:2187.
[10] Starkey SR, Frech R. Electrochim Acta 1997;42:471.
[11] Huq R, Koksbang R, Tonder PE, Farrington GC. Electrochim Acta 1992;37:1681.
[12] Such K, Stevens JR, Wieczorek W, Siekiersk M, Florjanczyk Z. J Polym Sci Part B, Polym Phys 1994;32:2221.
[13] Abraham KM. Electrochim Acta 1993;38:1681.
[14] Abraham KM, Alamgir M. J Power Sour 1993;43–44:195.
[15] Suzuki M, Yoshida Y, Kobayashi S, Koyama T, Kimura M, Hanabusa K, Shirai H. PCCP 1999;1:2749.
[16] Suzuki M, Yoshida Y, Koyama T, Kobayashi S, Kimura M, Hanabusa K, Shirai H. Polymer 2000;41:4531.
[17] Watanabe M, Rikukawa M, Sanui K, Ogata N. J Appl Phys 1985;58:736.
[18] Delmas C, Braconnier JJ, Borthomieu Y, Hagenmuller P. Mat Res Bull 1978;22:741.
[19] Faure C, Delmas C, Eilmann P. J Power Sour 1991;36:497.
[20] Suzuki M, Takada N, Koyama T, Kobayashi S, Kimura M, Hanabusa K, Shirai H, Miyata S. Chem Lett 2000:92.
[21] Williams ML, Landel RF, Ferry JD. J Am Chem Soc 1955;77:371.
[22] Fontanella JJ, Wintersgill MC, Smith MK, Semancik J. J Appl Phys 1986;60:2665.
[23] Kim JY, Kim SH. Solid State Ionics 1999;124:91.
[24] Chintapalli S, Frech R. Electrochim Acta 1998;43:1395.
[25] Noto VD, Longo D, Münchow V. J Phys Chem B 1999;103:2636.